

Radiative corrections to the magnetic-dipole transition amplitude in B-like ions

A. V. Volotka,^{1,2} D. A. Glazov,² G. Plunien,¹ V. M. Shabaev,² and I. I. Tupitsyn²

¹ *Institut für Theoretische Physik,*

Technische Universität Dresden,

Mommsenstraße 13,

D-01062 Dresden, Germany

² *Department of Physics,*

St. Petersburg State University,

Oulianovskaya 1, Petrodvorets,

198504 St. Petersburg, Russia

Abstract

The one-electron quantum-electrodynamic corrections to the magnetic-dipole transition amplitude between the fine-structure levels $(1s^2 2s^2 2p)^2 P_{3=2}$ $^2 P_{1=2}$ in boronlike ions are calculated to all orders in Z^{-1} . The results obtained serve for improving the theoretical accuracy of the lifetime of the $(1s^2 2s^2 2p)^2 P_{3=2}$ level in boronlike argon.

PACS numbers: 31.30 Jv, 32.70 Cs

I. INTRODUCTION

The precision in measurements of decay rates of forbidden transitions has considerably increased during the last years [1, 2, 3, 4, 5, 6, 7]. The accuracy achieved for the magnetic-dipole (M1) transition $(1s^2 2s^2 2p)^2 P_{3=2} \rightarrow 2P_{1=2}$ in B-like Ar became better than one part per thousand [6, 7]. This experimental precision demands a corresponding increase in the accuracy of the theoretical predictions. In a recent work [8] we have calculated the M1-transition probabilities between the fine-structure levels in B- and Be-like ions within the region of nuclear charge numbers $Z = 16 - 22$. In particular, it was found that the theoretical result for the case of Ar^{13+} deviates from the experimental one by about 3 %.

In Ref. [8], the relativistic, interelectronic-interaction, and quantum-electrodynamic (QED) corrections to the M1-transition amplitude were computed, while experimental values were taken for the transition energies. The configuration-interaction method in the Dirac-Fock-Sturm basis (CIDFS) was employed in order to evaluate the interelectronic-interaction contribution. Corrections due to single excitations to the negative-continuum energy states were taken into account in the many-electron wave functions. As it is known from [9, 10], such corrections may be significant in calculations involving operators, which mix large and small components of the wave functions, such as the M1-transition operator. The frequency-dependent term (consult the detailed description presented in Ref. [11]) was calculated within perturbation theory to first order in $1/Z$. The QED correction was obtained within leading order by including the electron anomalous magnetic moment (EAMM) in the M1-transition operator. Uncalculated higher-order QED terms together with the experimental errors of the transition energy determine the total uncertainty of the theoretical predictions presented in Ref. [8]. In this work, which is aiming for improvements of the evaluation of the radiative effects to the M1-transition probability in B-like ions, we present the exact calculation of the one-electron QED corrections going beyond the EAMM approximation.

Accordingly, the bound-electron propagator is treated exactly. This approach was already employed for the evaluation of the radiative corrections to the decays $2P_{1=2}; 2S; 2P_{3=2} \rightarrow 1s$ in hydrogenic ions [12] and parity nonconserving transitions in neutral Cs and Fr [13, 14]. Besides, in Ref. [15] the QED corrections to the transition probability between the hyperfine-structure components were expressed in terms of the corresponding corrections to the bound-electron g factor. The latter ones were calculated to all orders in $1/Z$ for the $1s$ and $2s$ states in Refs. [16, 17, 18, 19, 20].

Relativistic units ($\hbar = c = m = 1$) and the Heaviside charge unit [$\mu_0 = e^2 = (4\pi); e < 0$] are

used throughout the paper.

II. BASIC FORMULAS

The magnetic-dipole transition probability between the one-electron states a and b can be written in the form

$$W_D = \frac{2}{2j_a + 1} \sum_{m_a} \sum_{m_b} \sum_M |A_{1M}|^2; \quad (1)$$

where the summation over the photon polarization and the integration over the photon energy and angles were carried out. The initial state a is characterized by the angular momentum j_a , its projection m_a , and the energy ϵ_a , while the final state b has the corresponding quantum numbers j_b , m_b , and the energy ϵ_b . The transition amplitude A_{1M} is defined by

$$A_{1M} = \frac{r}{3!} \langle b | T_M^1 | a \rangle; \quad (2)$$

where ω is the transition energy and T_M^1 denote the spherical components of the M1-transition operator

$$T^1 = \frac{e}{2} \mathbf{j}_1(\omega r) \frac{[\mathbf{r}]}{r}; \quad (3)$$

Here j_1 denotes the first-order spherical Bessel function and \mathbf{r} is the Dirac-matrix vector. In further calculations we take into account only the first term in the power expansion of $j_1(\omega r)$, since for the case under consideration the transition wavelength is much larger than a typical ion size. Accordingly, the M1-transition operator T^1 can be related to the magnetic moment operator $\mu = e [\mathbf{r} \times \mathbf{p}]$,

$$T^1 = \frac{e}{3} \frac{\mathbf{p} \times \mathbf{r}}{2} = \frac{e}{3} \mu; \quad (4)$$

Utilizing the Wigner-Eckart theorem, the transition probability can be expressed in terms of the reduced matrix element of T_M^1 (see, e.g., Ref. [21]), which does not depend on the momentum projection M . Therefore, it is sufficient to calculate the transition amplitude for a given projection M only. In what follows we take $M = 0$ and omit the corresponding subscript.

In this work we focus on the one-loop QED contributions to the transition amplitude beyond the EAMM approximation. The vacuum-polarization (VP) and self-energy (SE) corrections, which one needs to consider, are diagrammatically depicted in Figs. 1 and 2, respectively. The VP

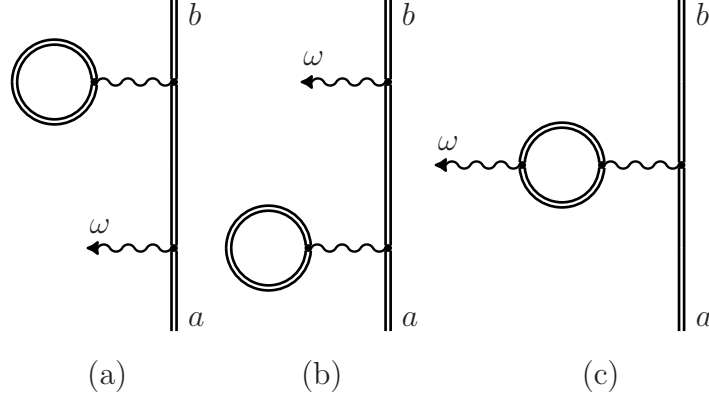


FIG. 1: Feynman diagrams representing the one-loop vacuum-polarization correction to the transition amplitude. The double line indicates the electron propagating in the external field of the nucleus. The photon propagator is represented by the wavy line, while the single photon emission is depicted by the wavy line with arrow.

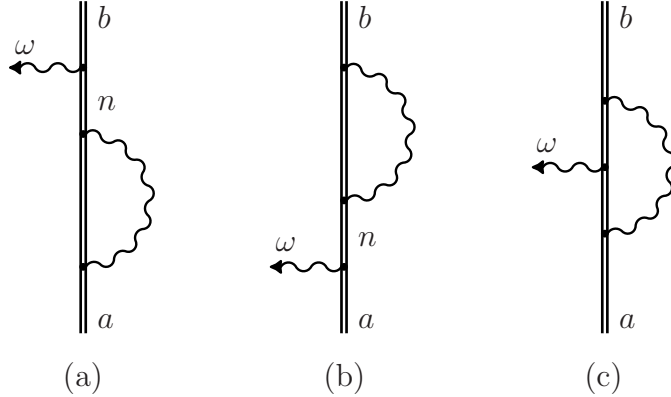


FIG. 2: Feynman diagrams representing the one-loop self-energy correction to the transition amplitude. Notations are the same as in Fig. 1.

correction corresponding to the diagrams presented in Figs. 1(a) and 1(b) (the electric-loop term) has been calculated in the Uehling potential approximation. The diagram depicted in Fig. 1(c) (the magnetic-loop term) has the magnetic-interaction insertion into the VP loop. It is known, that the contribution of this diagram vanishes in the Uehling approximation. The higher-orders VP terms turn out to be rather small and can be neglected. The remaining part of the work is devoted to the SE correction. Here we present the formal expressions for the corresponding contributions, which were derived at length in Ref. [22].

The contributions of the diagrams depicted in Figs. 2(a) and 2(b) are conveniently divided into

irreducible and reducible parts. The reducible (“red”) contribution of the diagram depicted in Fig. 2(a) is defined as a part in which the intermediate state energy $\epsilon_n = \epsilon_a$, respectively $\epsilon_n = \epsilon_b$ for the diagram presented in Fig. 2(b). The irreducible (“irr”) part is given by the remainder. The latter one can be written in terms of nondiagonal matrix elements of the self-energy operator (see, for details, Ref. [22])

$$A^{\text{irr}} = \frac{r}{3} \frac{2!^3}{3} (\langle b | j_R(\epsilon_b) | a \rangle + \langle b | j_R(\epsilon_a) | a \rangle); \quad (5)$$

where the perturbations to the wave functions are defined as

$$|j_a\rangle = \sum_n \frac{\langle n | j | a \rangle}{\epsilon_b - \epsilon_n}; \quad |j_b\rangle = \sum_n \frac{\langle n | j | b \rangle}{\epsilon_a - \epsilon_n}; \quad (6)$$

$j_R(\epsilon)$ is the renormalized self-energy insertion, which is related to the unrenormalized self-energy $j(\epsilon)$,

$$\langle a | j_R(\epsilon) | b \rangle = \frac{i}{2} \int_{-1}^1 dE \sum_n \frac{\langle a | j | n \rangle \langle n | j | b \rangle}{\epsilon - E - \epsilon_n(1 - i0)}; \quad (7)$$

by $j_R(\epsilon) = j(\epsilon) - \delta m$, where m is the mass counterterm. In Eq. (7) we use the following notations $\epsilon = (1; \mathbf{k})$, $I(E) = e^2 D(E)$, where $D(E)$ is the photon propagator. The expression for the reducible part is given by [22]

$$A^{\text{red}} = \frac{r}{6} \frac{2!^3}{6} \langle b | j_z | a \rangle (\langle a | j^0(\epsilon_a) | a \rangle + \langle b | j^0(\epsilon_b) | b \rangle); \quad (8)$$

where $j^0(\epsilon_a) = \langle a | j^0 | a \rangle = \langle a | j^0 | a \rangle$. The contribution of the diagram depicted in Fig. 2(c), known as the vertex (“ver”) term, is given by the equation [22]

$$A^{\text{ver}} = \frac{r}{3} \frac{2!^3}{3} \frac{i}{2} \int_{-1}^1 dE \sum_{n_1 n_2} \frac{\langle n_1 | j_z | n_2 \rangle \langle n_2 | j | a \rangle \langle a | j | n_1 \rangle}{(\epsilon_b - E - \epsilon_{n_1}(1 - i0))(\epsilon_a - E - \epsilon_{n_2}(1 - i0))}; \quad (9)$$

The irreducible part can be renormalized in the same manner as the ordinary SE correction to the energy. This renormalization is well-known and discussed in details in [23, 24, 25]. The ultraviolet divergence in the vertex and reducible contributions can be isolated by expanding the bound-electron propagator in terms of the interaction with the field of the nucleus. For our purposes, it is convenient to decompose the total contribution into zero-, one-, and many-potential terms according to the number of interactions with the external field

$$A^{\text{ver}} = A^{\text{ver}(0)} + A^{\text{ver}(1)} + A^{\text{ver}(2+)} \quad (10)$$

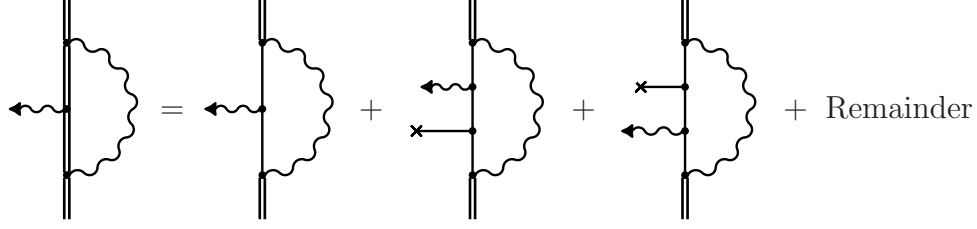


FIG. 3: The potential expansion of the vertex diagram. The single line indicates the free-electron propagator and the line ending with the cross denotes the interaction with the field of the nucleus. All higher-order contributions are contained in the Remainder.

and

$$A^{\text{red}} = A^{\text{red}(0)} + A^{\text{red}(1)} + A^{\text{red}(2+)} ; \quad (11)$$

This expansion for the vertex diagram is schematically presented in Fig. 3. In order to remove the divergences in the vertex and reducible terms, we consider them together. Combining the corresponding parts, we define

$$A^{\text{vr}(i)} = A^{\text{ver}(i)} + A^{\text{red}(i)} ; \quad (i = 0; 1; 2+) ; \quad (12)$$

It can be shown, that the ultraviolet-divergent terms, which are present in $A^{\text{ver}(0)}$ and $A^{\text{red}(0)}$, cancel each other in $A^{\text{vr}(0)}$. The remaining one- and many-potential terms are ultraviolet finite.

The zero- and one-potential contributions are evaluated in momentum space, while the many-potential term is calculated in the coordinate space employing the partial-wave expansion. The scheme for the separate treatment of the one-potential term was also used in previous g factor calculations presented in Refs. [17, 18, 19, 20]. It improves considerably the convergence of the partial-wave expansion in the low and middle Z region. The summarized expressions for the reducible correction are similar to those derived for the g factor (see, Ref. [20]). However, for the vertex contribution there are some principal differences. In contrast to Eq. (4) of Ref. [20], two different energies ϵ_a and ϵ_b enter the denominator of formula (9) and the matrix element $\langle \chi_{n_2} | \mathbf{J}(\mathbf{E}) | \chi_{n_1} \rangle$ depends on both states a and b. Taking these differences into account, we derive the corresponding formulas for the $A^{\text{ver}(0)}$ term in the Appendix. The derivation of the formulas for the one-potential vertex contribution is somewhat more complicated. However, taking the energy to be the same for both electron propagators (e.g., ϵ_a), the expressions for $A^{\text{ver}(1)}$ can be obtained in the same manner as for the g factor [20]. The remaining many-potential term can be

evaluated by the point-by-point subtraction of the corresponding zero- and one-potential contributions in the coordinate space. Consistently, we subtract the one-potential vertex contribution with the same energy variable in the electron propagators as it is taken in the $A^{\text{ver}(1)}$ term calculated in the momentum space. Furthermore, the term with $n_1 = n_b$ and $n_2 = n_a$ in Eq. (9) has an infrared divergence, which is canceled by the corresponding term of the reducible contribution.

For the numerical evaluation we employ the finite-basis-set method for the Dirac equation constructed via the dual kinetic balance approach [26]. The summation of the partial-wave expansion was performed up to $j_{\text{max}} = 10$, while the remaining tail was approximated by a least-square inverse-polynomial fitting.

III. RESULTS AND DISCUSSION

The one-loop QED corrections beyond the electron anomalous magnetic moment approximation are conveniently expressed in terms of the correction δ , which is defined through

$$A_{\text{QED}} = A_{\text{nr}} (2\delta_e + \dots); \quad (13)$$

where A_{nr} is the nonrelativistic transition amplitude and

$$\delta_e = \frac{\alpha}{2} (0.328478965 \dots) - \frac{\alpha^2}{\pi} + \dots \quad (14)$$

represents the electron anomalous magnetic factor corresponding to the EAMM term. In Table I we present our results for the one-electron SE correction. The VP term calculated within the Uehling approximation has been found to be negligible. The various contributions corresponding to the SE corrections to the transition amplitude are given in Table I. The one- and many-potential terms are represented as the sum $\text{vr}(1+) = \text{vr}(1) + \text{vr}(2+)$. As one can see from this table, the occurring cancellation reduces the total value for the correction δ by an order of magnitude compared to the individual terms. Most serious computational difficulties arise from the extrapolation of the partial-wave expansion of the many-potential term. In order to estimate the error, we perform a second evaluation of $\text{vr}(1+)$ without separating out the one-potential term. The difference between the results of both calculations is taken for the uncertainty.

The obtained results allow for an improvement of the theoretical values of the M1-transition probabilities between the states $(1s^2 2s^2 2p)^2 P_{3=2} \rightarrow ^2 P_{1=2}$ in B-like ions presented in [8]. In Table II the results of the CIDFS calculation without the QED term W^0 [8], the improved radiative

TABLE I: Individual contributions to the one-electron self-energy correction expressed in terms of the various corrections, defined by equation (13). Numbers in parenthesis represent error in the last digit.

Z	irr	$v_{r(0)}$	$v_{r(1+)}$	
16	0.0177	0.0124	0.0065(1)	0.0012(1)
17	0.0195	0.0136	0.0075(1)	0.0016(1)
18	0.0213	0.0148	0.0084(1)	0.0019(1)
19	0.0232	0.0160	0.0094(1)	0.0022(1)
20	0.0252	0.0172	0.0105(1)	0.0025(1)
21	0.0272	0.0185	0.0116(1)	0.0029(1)
22	0.0292	0.0197	0.0128(1)	0.0033(1)

correction W_{QED} , the total values of the transition probability W_{total} and the lifetime τ_{total} are compiled. For the transition energies we used the experimental values from Refs. [27, 28]. They are presented in the second column of Table II. For S^{11+} , Cl^{12+} , K^{14+} , and Ti^{17+} the uncertainties of the values of W_{total} and τ_{total} are determined by the errors in the experimental transition energies. Thus the accuracy of the total results for these ions has not been improved in comparison with the values presented in Ref. [8]. However, for Ar^{13+} the experimental value for the transition energy is known with high precision [28] and the uncertainty of the predictions obtained in Ref. [8] is determined by the uncalculated QED terms beyond the EAMM approximation. The present calculation of the radiative correction W_{QED} has improved the accuracy of the total values of the transition probability W_{total} and the lifetime τ_{total} for Ar^{13+} by an order of magnitude. Furthermore, for argon ion we have added the probability of the electric-quadrupole mode $W_{\text{E}2} = 0.00194 \text{ s}^{-1}$ calculated in Coulomb gauge in Ref. [29] to the total decay rate and lifetime.

In Table II, we also compare our total results with corresponding experimental data. The disagreement with the most accurate experimental value for Ar^{13+} [6, 7] can be stated. The reason for this discrepancy is still unclear for us.

Acknowledgments

Valuable conversations with O. Yu. Andreev, A. N. Artemyev, D. A. Solovyev, and V. A. Yerokhin are gratefully acknowledged. This work was supported in part by RFBR (Grant No. 04-

TABLE II: The decay rates Γ [s^{-1}] of the transition $(1s^2 2s^2 2p)^2 P_{3=2} \rightarrow 2P_{1=2}$ and the lifetime τ [ms] of the $(1s^2 2s^2 2p)^2 P_{3=2}$ state in B-like ions. The transition energies are given in cm^{-1} . The values of Γ^0 are taken from Ref. [8]. Results of the present work Γ_{QED} , Γ_{total} and τ_{total} are given in columns 4 to 6. For comparison, the experimental values τ_{expt} are presented in the last column. Numbers in parenthesis denote the estimated uncertainty.

Ions	Energy and Ref.	Γ^0 [8]	Γ_{QED}	Γ_{total}	τ_{total}	τ_{expt} and Ref.
S ¹¹⁺	13135(1) [27]	20.34481	0.09444	20.439(5)	48.93(1)	
Cl ¹²⁺	17408(20) [27]	47.34975	0.21972	47.57(16)	21.02(7)	21.2(6) [5] 21.1(5) [5]
Ar ¹³⁺	22656.22(1) [28]	104.36006	0.48419	104.846(3)	9.5378(3)	9.12(18) [1] 9.70(15) [3] 9.573(4)(5) [6]
K ¹⁴⁺	29006(25) [27]	218.9394	1.0156	220.0(6)	4.546(12)	4.47(10) [4]
Ti ¹⁷⁺	56243(4) [27]	1594.714	7.393	1602.1(5)	0.6242(2)	0.627(10) [2]

02-17574) and by INTAS-GSI (Grant No. 03-54-3604). A.V.V. and G.P. acknowledge financial support from the GSI F+E program, DFG, and BMBF. D.A.G. acknowledges the support by the ‘‘Dynasty’’ foundation.

Appendix: Zero-potential vertex term

Let us start from the momentum representation of the transition amplitude A_{1M} . Referring to Eqs. (2) and (4) it can be written as

$$A_{1M} = \frac{r}{6} \frac{Z}{i\epsilon} \frac{d\mathbf{p} d\mathbf{p}^0}{(2\pi)^3} \bar{u}_b(\mathbf{p}) \gamma^0 u_a(\mathbf{p}^0); \quad (15)$$

where the gradient $\nabla_{\mathbf{p}^0}$ acts only on the $u_a(\mathbf{p}^0)$ function. In order to obtain the zero-potential vertex term $A^{\text{ver}(0)}$, we substitute $\bar{u}_b(\mathbf{p})$ by the renormalized part of the free-electron vertex operator

$$\bar{u}_b(\mathbf{p}; \mathbf{p}^0)$$

$$A^{\text{ver}(0)} = \frac{r}{6} \frac{Z}{i\epsilon} \frac{d\mathbf{p} d\mathbf{p}^0}{(2\pi)^3} \bar{u}_b(\mathbf{p}; \mathbf{p}^0) \gamma^0 u_a(\mathbf{p}^0); \quad (16)$$

In contrast to the g factor (see Eq. (15) of Ref. [20]), the wave functions of the initial (a) and final (b) states enter into Eq. (16) and $\chi_R(\mathbf{b};\mathbf{p};\mathbf{a};p^0)$ has different energy arguments. Integrating by parts and performing the integration over p^0 yields

$$A^{\text{ver}(0)} = \int_Z \frac{d^3p}{6} i e \frac{Z}{(2)^3} \chi_b(\mathbf{p}) \chi_a(\mathbf{p}) \chi_R(\mathbf{b};\mathbf{p};\mathbf{a};p) \chi_a(\mathbf{p}) ; \quad (17)$$

where

$$\chi(\mathbf{b};\mathbf{a};\mathbf{p}) = \int_{p^0} \chi_R(\mathbf{b};\mathbf{p};\mathbf{a};p^0) \chi_{p^0} : \quad (18)$$

The right side of Eq. (17) is naturally divided into two parts $A^{\text{ver}(0);1}$ and $A^{\text{ver}(0);2}$. Starting with the first one, it is convenient to represent the function $\chi(\mathbf{b};\mathbf{a};\mathbf{p})$ in the form

$$\chi(\mathbf{b};\mathbf{a};\mathbf{p}) = 4i \int_Z \frac{d^4k}{(2)^4 k^2} \frac{\mathcal{P}(\mathbf{k} + \mathbf{m})}{(\mathbf{p} - \mathbf{k})^2 m^2} \left[\chi_R(\mathbf{p}) \chi_Z \frac{\mathcal{P}^0(\mathbf{k} + \mathbf{m})}{(\mathbf{p}^0 - \mathbf{k})^2 m^2} \right] \quad (19)$$

with $\mathbf{p} = (\mathbf{b};\mathbf{p})$, $\mathbf{p}^0 = (\mathbf{a};\mathbf{p})$, and $\mathcal{P} = \mathbf{p}$, respectively. Using the commutation identity for the γ matrices, we get

$$\chi(\mathbf{b};\mathbf{a};\mathbf{p}) = \frac{1}{4i^3} \int_Z \frac{d^4k}{k^2} \frac{1}{[(\mathbf{p} - \mathbf{k})^2 m^2][(\mathbf{p}^0 - \mathbf{k})^2 m^2]} (\mathcal{P} - \mathbf{k} + \mathbf{m}) \left[\chi_R(\mathbf{p}) \chi_Z \frac{(\mathcal{P}^0 - \mathbf{k} + \mathbf{m})}{(\mathbf{p}^0 - \mathbf{k})^2 m^2} \right] ; \quad (20)$$

Expressing the integration over the loop momenta k in terms of the integrals over the Feynman parameters, one can derive the formula

$$\chi(\mathbf{b};\mathbf{a};\mathbf{p}) = -i \int_0^1 \int_0^1 \int_0^1 (C_0 + C_{11} + C_{12}) \mathcal{P} \mathcal{P}^0 (A_0 - A_1) \mathcal{P} (A_0 + 3A_1) + 2p^2 (A_{11} - A_{21}) + 2p^{02} (A_{12} - A_{22}) - 4p^0 p^2 A_{23} \left[\chi_R(\mathbf{p}) \chi_Z \right] ; \quad (21)$$

which coincides with the corresponding equation in calculations of the g factor, if one considers $\mathbf{a} = \mathbf{b}$. Here the Feynman integrals are determined as

$$C_0 = \int_0^1 \frac{dy}{(yp + (1-y)p^0)^2} (\ln X) ; \quad (22)$$

$$\frac{C_{11}}{C_{12}} = \int_0^1 \frac{dy}{(yp + (1-y)p^0)^2} \frac{y}{1-y} (\ln X) ; \quad (23)$$

$$A_0 = \int_0^Z \int_0^1 dx dy \frac{(1-x)(1-y)}{Z^2}; \quad (24)$$

$$A_1 = \int_0^Z \int_0^1 dx dy \frac{x(1-x)(1-y)}{Z^2}; \quad (25)$$

$$A_{11} = \int_0^Z \int_0^1 dx dy \frac{x(1-x)(1-y)}{Z^2} y; \quad (26)$$

$$A_{21} = \int_0^Z \int_0^1 dx dy \frac{x^2(1-x)(1-y)}{Z^2} y^2; \quad (27)$$

and

$$x = 1 + \frac{1}{Y}; \quad (28)$$

$$Y = \frac{1 - Yp^2 - (1 - Y)p^{02}}{(Yp + (1 - Y)p^0)^2}; \quad (29)$$

$$Z = x [Yp + (1 - Y)p^{02}] + 1 - Yp^2 - (1 - Y)p^{02}.$$

To carry out the angular integration for the transition under consideration $2p_{3=2} \rightarrow 2p_{1=2}$ we employ the following results for basic integrals ($\ell = 1=2$)

$$\int d p_{\ell}^y \int d p_{\ell}^z \int d \hat{\rho} = \begin{cases} 2^{\ell} \frac{p_{\ell}^{\ell}}{2=3} \text{ for } \ell_1 = 1; \ell_2 = 2; \\ 0 \text{ for } \ell_1 = 1; \ell_2 = 2; \end{cases} \quad (30)$$

$$\int d p_{\ell}^y \int d p_{\ell}^z \int d \hat{\rho} [\hat{\rho}_k \hat{\rho}_{\ell}] = \begin{cases} p_{\ell}^{\ell} \frac{p_{\ell}^{\ell}}{2=3 i} \text{ for } \ell_1 = 1; \ell_2 = 2; \\ p_{\ell}^{\ell} \frac{p_{\ell}^{\ell}}{2=3 i} \text{ for } \ell_1 = 1; \ell_2 = 2; \end{cases} \quad (31)$$

where $\hat{\rho} = p = \hat{p} \hat{j}$ ($\hat{\rho}$) is the spherical spinor, and $\hat{\rho}_k$ denotes the vector of Pauli matrices.

Finally, for the first part $A^{\text{ver}(0);1}$ we obtain

$$A^{\text{ver}(0);1} = \frac{r}{3} \frac{e}{24^4} \int_0^Z \int_0^1 d p_r p_r^2 \left[2(C_0 + C_{11} + C_{12}) (\mathbf{g}_b \mathbf{g}_a + p_r \mathbf{g}_b \mathbf{f}_a) + p_r (\mathbf{f}_a \mathbf{f}_b - p_r^2) (A_0 - A_1 - 4A_{23}) + (A_0 + 3A_1) + 2(\mathbf{f}_b^2 - p_r^2) (A_{11} - A_{21}) + 2(\mathbf{f}_a^2 - p_r^2) (A_{12} - A_{22}) + (\mathbf{g}_b \mathbf{f}_a - \mathbf{f}_b \mathbf{g}_a) \right] p_r^2 (\mathbf{f}_a \mathbf{f}_b) (A_0 - A_1) (\mathbf{g}_b \mathbf{g}_a - \mathbf{f}_b \mathbf{f}_a); \quad (32)$$

where $p_r = \hat{p} \cdot \hat{g}_a(p_r)$ and $f_a(p_r)$ are the upper and lower radial components of the wave function in the momentum representation, respectively.

The second term $A^{\text{ver}(0);2}$ can be calculated similarly. Using the expression for the free-electron vertex function [25] and employing in addition to Eq. (31) the following angular integrals

$$\int_0^Z d p_y \frac{y}{p} (\hat{\phi}) \int_0^p r_p \frac{z}{p} (\hat{\phi}) = \begin{cases} p \frac{z}{2} = 3i \text{ for } \phi_1 = 1; \phi_2 = 2; \\ 0 \text{ for } \phi_1 = 1; \phi_2 = 2; \end{cases} \quad (33)$$

$$\int_0^Z d p_y \frac{y}{p} (\hat{\phi}) \int_0^p r_p \frac{z}{p} (\hat{\phi}) = \begin{cases} 2 \frac{p}{2} = 3i \text{ for } \phi_1 = 1; \phi_2 = 2; \\ p \frac{z}{2} = i \text{ for } \phi_1 = 1; \phi_2 = 2; \end{cases} \quad (34)$$

where r_p is the angular part of the gradient, we have

$$\begin{aligned} A^{\text{ver}(0);2} = & \frac{r}{3} \frac{1}{96} \frac{e}{4} \int_0^Z \frac{1}{p_r^2} dp_r p_r^2 (A \mu_a \mu_b D + p_r^2 D) (g_b f_a^0 - f_b g_a^0 \\ & + \frac{3}{p_r} g_b f_a - \frac{2}{p_r} f_b g_a) p_r D (\mu_a - \mu_b) (f_b f_a^0 - g_b g_a^0 + \frac{3}{p_r} f_b f_a - \frac{2}{p_r} g_b g_a) \\ & + (\mu_b B + 2 \mu_b D + \mu_a C + 4D) g_b g_a + p_r (B + 2D + C) f_b g_a ; \end{aligned} \quad (35)$$

where $g_a^0(p_r) = dg_a(p_r) = dp_r$, $f_a^0(p_r) = df_a(p_r) = dp_r$. Here the set of coefficients are expressed in terms of the Feynman integrals as

$$A = C_{24} \frac{2}{3} + (\mu_b^2 - p_r^2) C_{11} + (\mu_a^2 - p_r^2) C_{12} + 4(\mu_a \mu_b - p_r^2) (C_0 + C_{11} + C_{12}) \\ 2C_0 + C_{11} + C_{12} ; \quad (36)$$

$$B = 4(C_0 + 2C_{11} + C_{12} + C_{21} + C_{23}) ; \quad (37)$$

$$C = 4(C_0 + C_{11} + 2C_{12} + C_{22} + C_{23}) ; \quad (38)$$

$$D = 2(C_0 + C_{11} + C_{12}) ; \quad (39)$$

and

$$C_{24} = \int_0^Z dy \ln(y^2 (\mu_a - \mu_b)^2 - y(\mu_a - \mu_b)^2 + 1) ; \quad (40)$$

The total result for the zero-potential vertex contribution is the sum of the corresponding terms from Eqs. (32) and (35).

- [1] D. P. Moehs and D. A. Church, *Phys. Rev. A* **58**, 1111 (1998).
- [2] E. Träbert, G. Gwinner, A. Wolf, X. Tordoir, and A. G. Calamai, *Phys. Lett. A* **264**, 311 (1999).
- [3] E. Träbert, P. Beiersdorfer, S. B. Utter, G. V. Brown, H. Chen, C. L. Harris, P. A. Neill, D. W. Savin, and A. J. Smith, *Astrophys. J.* **541**, 506 (2000).
- [4] E. Träbert, P. Beiersdorfer, G. V. Brown, H. Chen, E. H. Pinnington, and D. B. Thorn, *Phys. Rev. A* **64**, 034501 (2001).
- [5] E. Träbert, P. Beiersdorfer, G. Gwinner, E. H. Pinnington, and A. Wolf, *Phys. Rev. A* **66**, 052507 (2002).
- [6] A. Lapiere, U. D. Jentschura, J. R. Crespo López-Urrutia, J. Braun, G. Brenner, H. Bruhns, D. Fischer, A. J. González Martínez, Z. Harman, W. R. Johnson, C. H. Keitel, V. Mironov, C. J. Osborne, G. Sikler, R. Soria Orts, V. M. Shabaev, H. Tawara, I. I. Tupitsyn, J. Ullrich, and A. V. Volotka, *Phys. Rev. Lett.* **95**, 183001 (2005).
- [7] A. Lapiere, J. R. Crespo López-Urrutia, J. Braun, G. Brenner, H. Bruhns, D. Fischer, A. J. González Martínez, V. Mironov, C. J. Osborne, G. Sikler, R. Soria Orts, H. Tawara, J. Ullrich, V. M. Shabaev, I. I. Tupitsyn, and A. V. Volotka, to be published.
- [8] I. I. Tupitsyn, A. V. Volotka, D. A. Glazov, V. M. Shabaev, G. Plunien, J. R. Crespo López-Urrutia, A. Lapiere, and J. Ullrich, *Phys. Rev. A.* **72**, 062503 (2005).
- [9] P. Indelicato, *Phys. Rev. Lett.* **77**, 3323 (1996).
- [10] A. Derevianko, I. M. Savukov, W. R. Johnson, and D. R. Plante, *Phys. Rev. A* **58**, 4453 (1998).
- [11] P. Indelicato, V. M. Shabaev, and A. V. Volotka, *Phys. Rev. A* **69**, 062506 (2004).
- [12] J. Sapirstein, K. Pachucki, and K. T. Cheng, *Phys. Rev. A* **69**, 022113 (2004).
- [13] V. M. Shabaev, K. Pachucki, I. I. Tupitsyn, and V. A. Yerokhin, *Phys. Rev. Lett.* **94**, 213002 (2005).
- [14] V. M. Shabaev, I. I. Tupitsyn, K. Pachucki, G. Plunien, and V. A. Yerokhin, *Phys. Rev. A.* **72**, 062105 (2005).
- [15] V. M. Shabaev, *Can. J. Phys.* **76**, 907 (1998).
- [16] S. A. Blundell, K. T. Cheng, and J. Sapirstein, *Phys. Rev. A* **55**, 1857 (1997).
- [17] H. Persson, S. Salomonson, P. Sunnergren, and I. Lindgren, *Phys. Rev. A* **56**, R2499 (1997).
- [18] T. Beier, I. Lindgren, H. Persson, S. Salomonson, P. Sunnergren, H. Häffner, and N. Hermanspahn, *Phys. Rev. A* **62**, 032510 (2000).
- [19] V. A. Yerokhin, P. Indelicato, and V. M. Shabaev, *Phys. Rev. Lett.* **89**, 143001 (2002).
- [20] V. A. Yerokhin, P. Indelicato, and V. M. Shabaev, *Phys. Rev. A* **69**, 052503 (2004).

- [21] I. I. Sobelman, *Atomic Spectra and Radiative Transitions*, (Springer, New York, 1979).
- [22] V. M. Shabaev, Phys. Rep. **356**, 119 (2002).
- [23] N. J. Snyderman, Ann. Phys. (N.Y.) **211**, 43 (1991).
- [24] S. A. Blundell and N. J. Snyderman, Phys. Rev. A **44**, R1427 (1991).
- [25] V. A. Yerokhin and V. M. Shabaev, Phys. Rev. A **60**, 800 (1999).
- [26] V. M. Shabaev, I. I. Tupitsyn, V. A. Yerokhin, G. Plunien, and G. Soff, Phys. Rev. Lett. **93**, 130405 (2004).
- [27] B. Edlén, Phys. Scripta **28**, 483 (1983).
- [28] I. Draganić, J. R. Crespo López-Urrutia, R. DuBois, S. Fritzsche, V. M. Shabaev, R. Soria Orts, I. I. Tupitsyn, Y. Zou, and J. Ullrich, Phys. Rev. Lett. **91**, 183001 (2003).
- [29] K. Koc, J. Phys. B **36**, L93 (2003).